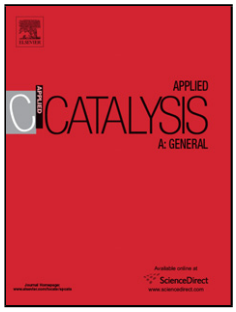

Title: Synthesis of new metalloporphyrin derivatives from [5,10,15,20-tetrakis (pentafluorophenyl)porphyrin] and 4-mercaptobenzoic acid for homogeneous and heterogeneous catalysis

Author: Kelly A.D.deF. Castro MárioM.Q. Simõ es Maria da Graça P.M.S. Neves JoséA.S. Cavaleiro Ronny R. Ribeiro Fernando Wypych Shirley Nakagaki

PII: S0926-860X(14)00810-2
DOI: http://dx.doi.org/doi:10.1016/j.apcata.2014.12.048
Reference: APCATA 15187

To appear in: *Applied Catalysis A: General*

Received date: 7-11-2014
Revised date: 18-12-2014
Accepted date: 25-12-2014

Please cite this article as: K.A.D.F. Castro, M.M.Q. Simõ es, M.G.P.M.S. Neves, J.A.S. Cavaleiro, R.R. Ribeiro, F. Wypych, S. Nakagaki, Synthesis of new metalloporphyrin derivatives from [5,10,15,20-tetrakis (pentafluorophenyl)porphyrin] and 4-mercaptobenzoic acid for homogeneous and heterogeneous catalysis, *Applied Catalysis A, General* (2015), http://dx.doi.org/10.1016/j.apcata.2014.12.048

Highlights

Synthesis of new metalloporphyrin derivatives from [5,10,15,20-tetrakis (pentafluorophenyl)porphyrin] and 4-mercaptobenzoic acid for homogeneous and heterogeneous catalysis

1- Porphyrins preparation via [H_2(TFPP)] structural modification with mercaptobenzoic acid.

2- The substituent groups in the new porphyrins furnished structured solids.

3- New insoluble metalloporphyrins derivatives as catalysts in heterogeneous medium.

4- New metalloporphyrin derivatives as catalyst in the oxidation of alkenes and alkanes.

5- New insoluble metalloporphyrin catalyst and its reuse capacity in oxidation reaction.

Manuscript before reviewer's suggestions

Synthesis of new metalloporphyrin derivatives from [5,10,15,20-tetrakis (pentafluorophenyl)porphyrin] and 4-mercaptobenzoic acid for homogeneous and heterogeneous catalysis

Kelly A. D. de F. Castro[1,2], Mário M. Q. Simões[2], Maria da Graça P. M. S. Neves[2,*], José A. S. Cavaleiro[2], Ronny R. Ribeiro[1], Fernando Wypych[1], Shirley Nakagaki[1,*]

[1]*Laboratório de Química Bioinorgânica e Catálise; Universidade Federal do Paraná (UFPR), CP 19081, CEP 81531-990, Curitiba, Paraná, Brazil.*

[2]*Department of Chemistry and QOPNA, University of Aveiro, 3810-193 Aveiro, Portugal.*

** Corresponding authors: e-mail address: shirleyn@ufpr.br; gneves@ua.pt*

Abstract

Inspired by the efficiency and selectivity of the reactions catalyzed by cytochrome P-450, in recent years researchers have made great efforts to develop synthetic routes that afford new porphyrins with different structures. Synthetic metalloporphyrins are catalysts that can efficiently insert oxygen and other atoms such as nitrogen and sulfur in hydrocarbons and in a wide variety of other organic compounds. Several studies have shown that second-generation metalloporphyrins, which bear electronegative and/or bulky substituents at the *meso* positions of the porphyrin ring, are more robust and resist to prevent degradation during catalytic essays. This work reports on a synthetic strategy to prepare new metalloporphyrins via structural modification of [5,10,15,20-tetrakis (pentafluorophenyl) porphyrin], or [H_2(TPFPP)], with 4-

mercaptobenzoic acid; it also describes their characterization and catalytic activity. The substituent groups present in the structure of the resulting porphyrins furnished structured solids, which could potentially serve as catalysts in heterogeneous medium. Investigation of the catalytic activity of the new derivatives in the oxidation of (Z)-cyclooctene, cyclohexane, and heptane, under homogeneous conditions, and in the oxidation of (Z)-cyclooctene, in heterogeneous medium, proved that the new metalloporphyrins constituted excellent catalysts for (Z)-cyclooctene epoxidation. As for alkane oxidation, they selectively gave the corresponding alcohol in good yields.

Keywords: *porphyrin, 4-mercaptobenzoic acid, nucleophilic substitution, homogeneous and heterogeneous catalysis, oxidation.*

1. Introduction

The use of synthetic macrocycles as catalysts in oxidation reactions has generated great interest in bioinorganic chemistry [1,2], mainly when it comes to modeling the proven catalytic ability of biological systems like cytochrome P-450 and lignin peroxidases [3,4]. Researchers have successfully modulated the high selectivity and chemical efficiency of catalytic systems based on these two heme proteins they used synthetic metalloporphyrins bearing both simple and more sophisticated structures [5-16]. They have developed these synthetic catalytic systems [1,5,17,18] aiming to obtain complexes that can effectively generate compounds in much the same way as cytochrome P-450 enzymes do. Examples of such compounds are industrially important products like epoxides, alcohols, and acids; compounds of pharmaceutical interest, namely specific isomers with pharmacological activity, and high-purity precursors; and metabolites and drug analogs. To obtain the desired catalytic selectivity for certain products, high degree of sophistication may be necessary during the design of specific catalysts [1,17].

Work developed over the last 20 years has shown that catalysts based on Fe(III) and Mn(III) complexes of synthetic *meso*-tetraarylporphyrins are the most efficient and selective for oxidation reactions. The stereo-electronic features of the substituents present in the aryl groups of these complexes exert an important effect on the lifetime and reactivity of the active catalytic species in solution. These substituents can inhibit the formation of dimeric species and prevent the auto-oxidative destruction that inactivates the catalyst [5,12,19-23]. In fact, extensive investigations have revealed that complexes of halogenated *meso*-

tetraarylporphyrins are more robust and resistant to degradation by free radical attack than those containing electron-donating substituents. These systems constitute effective catalysts for the oxidative insertion of oxygen in organic compounds, namely hydrocarbons; they can also transfer an oxygen atom to sulfur- and nitrogen-containing substrates with great efficacy [3,24-30]. Additionally, the pharmaceutical industry has explored these systems to prepare oxidized metabolites from drugs [3]. In particular, the complexes of 5,10,15,20-tetrakis(pentafluorophenyl)porphyrin, [H_2(TPFPP)], an excellent template for further functionalization with nucleophiles [31-33], have found promising applications in catalysis [8,9,11,13,15,19,34] and in other areas [36-40]. It is easy to prepare catalytically active polymeric metalloporphyrins by reacting [H_2(TPFPP)] or the corresponding metal complexes with polyethylene glycol in the presence of sodium hydride using toluene as solvent [41]. The same template [H_2(TPFPP)] has been used to obtain derivatives with adequate amphiphilicity for application as photosensitizers that can photodynamically inactivate microorganisms [42,43].

Recently, we have reported that metalloporphyrins with appended ethylene glycol substituents efficiently catalyze (Z)-cyclooctene and cyclohexane oxidation under homogeneous and heterogeneous conditions [34].

Considering our research interest in the synthesis of efficient catalysts based on [H_2(TPFPP)] functionalization, here we report on the synthesis and catalytic activity of new metalloporphyrins obtained by structural modification of [H_2(TPFPP)] with 4-mercaptobenzoic acid. Depending on the number of *para*-fluorophenyl substituents that 4-mercaptobenzoic acid replaces during the synthesis, further metal insertion into the porphyrin complex will afford structured solids that are insoluble in

most of the tested solvents. We investigated the catalytic activity of the synthesized metallocomplexes in (Z)-cyclooctene, cyclohexane, and heptane oxidation under homogeneous and heterogeneous catalytic conditions. We also assessed solid/heterogeneous catalysts recovery and reuse in the case that (Z)-cyclooctene was the substrate.

2. Experimental section

All the chemicals used in this study were purchased from Aldrich, Sigma, or Merck and were of analytical grade. Iodosylbenzene (PhIO) was synthesized by hydrolysis of iodosylbenzenediacetate [44], and the obtained solid was carefully dried under reduced pressure and kept at 5 °C.

2.1. Synthesis of metalloporphyrins (see Figure 1 for abbreviations)

The synthesis of the new metalloporphyrins involved three steps:

*(i) Synthesis of Porphyrin P**1***: the porphyrin ligand was prepared as described in the literature [45,46].

(*ii) Synthesis of the free-base porphyrins P**2**, P**3**, P**4**, P**5**, and P**6** from reaction of 4-mercaptobenzoic acid with porphyrin P**1** (Figure 1):* In a round-bottom flask, 0.4 mmol of 4-mercaptobenzoic acid was dissolved in 15 mL of DMF containing 0.5 mL of pyridine. The reaction mixture was kept under magnetic stirring at room temperature for 30 min. Porphyrin P**1** (0.1 mmol) was added, and the reaction mixture was kept under magnetic stirring for 3 h and monitored by TLC. Then, the solvent was evaporated under reduced pressure, and the crude solid was purified by preparative

TLC (thin-layer chromatography - silica was the stationary phase, and chloroform/methanol (9:1 v/v) was the mobile phase). In this process, several fractions were separated and numbered from 1 to 5.

The first fraction was identified as porphyrin P**2** (19% yield)**,** m.p. > 300 °C. ^{1}H NMR: δ_H ppm (CD_3OD) 9.20 (broad, 8H, H-β), 8.07 (d, *J* = 9 Hz, 2H, S-C_6H_4-CO_2H), and 7.66 (d, *J* = 9 Hz, 2H, S-C_6H_4-CO_2H). ^{19}F NMR: δ_F ppm (CD_3OD) -188.35 to -188.17 (m, 6F, F-*meta*), -178.57 (t, *J* = 20.0 Hz, 3F, F-*para*), -163.67 (dd, *J* = 7.5 and 22.8 Hz, 6F, F-*ortho*), -162.80 (dd, *J* = 12.3 and 24.3 Hz, 2F, F-*meta*), and -158.51 (dd, *J* = 12.3 and 24.3 Hz, 2F, F-*ortho*). UV–VIS ($CHCl_3$) λ_{max}, nm (log ε): 414 (5.20), 506 (4.08), 584 (3.90). HRMS (FAB^+) m/z: calcd for $C_{51}H_{16}F_{19}N_4O_2S$ $(M+H)^+$: 1109.0685; found: 1109.0667. The second and third fractions were identified as porphyrins P**3** and P**4**. Porphyrin P**3** (17% yield)**,** m.p. > 300 °C. ^{1}H NMR: δ_H ppm (CD_3OD): 9.18 (broad, 8H, H-β), 8.08 (d, *J* = 8.4 Hz, 4H, S-C_6H_4-CO_2H), and 7.67 (d, *J* = 8.4 Hz, 4H, S-C_6H_4-CO_2H). ^{19}F NMR: δ_F ppm (CD_3OD) -188.67 to -188.49 (m, 4F, F-*meta*), -179.01 (t, *J* = 20.4 Hz, 2F, F-*para*), -163.73 (dd, *J* = 7.8 and 23.0 Hz, 4F, F-*ortho*), -162.89 (dd, *J* = 12.2 and 24.4 Hz, 4F, F-*meta*), and -158.68 (dd, *J* = 12.2 and 24.4 Hz, 4F, F-*ortho*). UV–vis ($CHCl_3$) λ_{max}, nm (log ε): 412 (5.24), 506 (4.06), 584 (3.90). HRMS (FAB+) m/z: calcd for $C_{58}H_{21}F_{18}N_4O_4S_2$ $(M+H)^+$: 1243.0711; found: 1243.0696. Porphyrin P**4** (12% yield)**,** m.p. > 300 °C. ^{1}H NMR: δ_H ppm (CD_3OD): 9.18 (broad, 8H, H-β), 8.08 (d, *J* = 8.2 Hz, 4H, S-C_6H_4-CO_2H), and 7.67 (d, *J* = 8.2 Hz, 4H, S-C_6H_4-CO_2H). ^{19}F NMR: δ_F ppm (CD_3OD) -190.20 to -190.03 (m, 4F, F-*meta*), -180.54 (t, *J* = 20.2 Hz, 2F, F-*para*), -165.27 (dd, *J* = 7.3 and 22.6 Hz, 4F, F-*ortho*), -164.41 (dd, *J* = 12.3 and 24.5 Hz, 4F, F-*meta*), and -158.68 (dd, *J* = 12.3 and 24.5

Hz, 4F, F-*ortho*). UV–vis ($CHCl_3$) λ_{max}, nm (log ε): 412 (5.22), 506 (4.08), 582 (3.66). HRMS (FAB^+) m/z: calcd for $C_{58}H_{21}F_{18}N_4O_4S_2$ $(M+H)^+$: 1243.0711; found: 1243.0675. The fourth fraction was identified as porphyrin P**5** (37% yield)**,** m.p. > 300 °C. ^1H NMR: δ_H ppm (CD_3OD): 9.24 (broad, 8H, H-β), 8.16 (d, *J* = 8.4 Hz, 6H, S-C_6H_4-CO_2H), and 7.75 (d, *J* = 8.4 Hz, 6H, S-C_6H_4-CO_2H). ^{19}F NMR: δ_F ppm (CD_3OD) -190.19 to -190.02 (m, 2F, F-*meta*), -180.53 (t, *J* = 20.4Hz, 1F, F-*para*), -165.25 (dd, *J* = 7.6 and 22.6 Hz, 2F, F-*ortho*), -164.40 to 164.21 (m, 4F, F-*meta*), and -160.20 (dd, *J* = 12.3 e 24.7 Hz, 4F, F-*ortho*). UV–VIS (CH_3OH) λ_{max}, nm (log ε): 410 (5.16), 504 (4.13), 582 (3.65). HRMS (FAB^+) m/z: calcd for $C_{65}H_{26}F_{17}N_4O_6S_3$ $(M+H)^+$: 1377.0738; found: 1377.0737. The protons signal relative to N-H was not observed, due to their replacement by deuterium from deuterated methanol in porphyrins P**2**-P**6**. Finally, the fifth fraction was identified as porphyrin P**6** (3.1% yield), m.p. > 300 °C, ^1H NMR: δ_H ppm (Acetone-d6) 9.46 (broad, 8H, H-β), 8.14 (d, *J* = 8.4 Hz, 8H, S-C_6H_4-CO_2H), 7.82 (d, *J* = 8.3 Hz, 8H, S-C_6H_4-CO_2H), and -2.87 (s, 2H, NH). ^{19}F NMR: δ_F ppm (Acetone-d6) -162.02 (dd, *J* = 11.9 and 24.7 Hz, 8F, F-*meta*), and -157.70 (dd, *J* = 11.9 and 24.7 Hz, 8F, F-*ortho*). UV–VIS (Acetone) λ_{max}, nm (log ε): 412 (5.14), 504 (4.07), 582 (3.57). HRMS (FAB+) m/z: calcd for $C_{72}H_{31}F_{16}N_4O_8S_4$ $(M+H)^+$: 1511.0764; found: 1511.0752.

The reaction yields described above were obtained after 3 h of reaction; when the reaction conducted under the same conditions was stopped after 1 h, the yield of porphyrin P**2** was higher 33.6%; porphyrins P**3** and P**4** were isolated in yields ranging from ca. 15 to 25%. To optimize the formation of porphyrin P**6**, the reaction was performed as described previously, but 0.72 mmol of 4-mercaptobenzoic acid, 15 mL

of DMF, 4.0 mL of pyridine, and 0.102 mmol of porphyrin P**1** were used instead. After 48 h of reaction, porphyrin P**6** was isolated in 96% yield.

*(iii) Preparation of manganese, iron, and copper porphyrins (MP**x**):* To insert a metal into the free-base porphyrins P**1**, P**2**, and P**6**, a modification of the conventional method described by Kobayashi[47] was employed. To obtain the iron complexes, the reactions were carried out using acetic acid (P**1**) or DMF (P**2** and P**6**) as solvent, iron(II) chloride, and sodium acetate (to aid deprotonation). The reactions were performed under reflux in argon atmosphere for 24 h, to yield FeP**1**, FeP**2**, and FeP**6** (confirmed by the observation of the characteristic bands by UV-VIS analyses), The argon atmosphere was removed and solution reaction was kept under magnetic stirring at reflux system to ensure the total oxidation of Fe (II) to Fe (III).

To achieve the manganese complexes, manganese(II) acetate was used in the same solvents used for iron(III) metallation process. The reaction was conducted for 8 h, to afford MnP**1**, MnP**2**, and MnP**6**. The oxidation of Mn(II) to Mn(III) was also performed in air as described for FeP.

Copper was also inserted into porphyrins P**1** and P**6**, using copper(II) acetate, DMF as solvent, and reaction time of 3 h, to give CuP**1** and CuP**6**. After metal insertion, the solvents were removed under vacuum. The resulting solids were thoroughly washed with water, to remove excess metal salts. The complexes were purified by column chromatography using dichloromethane as eluent. The preparation of CuP**2** was not performed in this stage, since the material amount (free base porphyrin) was insufficient.

During metal insertion into porphyrin P**6**, the corresponding metalloporphyrins (MnP**6**, FeP**6**, and CuP**6**) precipitated, and the resulting crude solids were insoluble in all the tested solvents. The other synthesized metalloporphyrins (CuP**1**, FeP**1**, FeP**2,** MnP**1**, and MnP**2**) behaved differently and the crude solids were soluble in different solvents and were purified by column chromatography.

2.2. Catalytic oxidation reactions

The following procedure was adopted to assess the oxidation of different substrates catalyzed by the previously prepared metalloporphyrins: about 1.0 mg of the metalloporphyrin was weighed in a 2-mL thermostatic glass reactor tube equipped with a magnetic stirrer. The reactor tube was placed inside a dark recipient, and iodosylbenzene was added, to obtain a 1:10 catalyst/oxidant molar ratio. The reactor was degassed with argon for 15 min, which was followed by addition of the solvent (acetonitrile, 400 μL) and the substrate ((Z)-cyclooctene, cyclohexane, or heptane). The oxidation reactions were carried out under magnetic stirring for 1 h or 24 h. (Z)-Cyclooctene had been previously purified by column chromatography on an alumina micro column. The reactions were quenched by addition of sodium sulfite saturated solution (approximately 0.1 mol/L), to eliminate excess PhIO. The reaction mixture was transferred to a volumetric flask, and aliquots were analyzed by gas chromatography after addition of the internal standard (a solution of 99.9% octan-1-ol in acetonitrile 1.0 x 10^{-2} mol/L). When the catalyst used in the reaction was insoluble (FeP**6**, MnP**6**, and CuP**6**), the solid catalyst was washed several times with methanol and acetonitrile after the reaction, to extract any reaction products that might have

adsorbed onto the solid. The washing solutions were added to the previously separated reaction supernatant, and the contents of these combined solutions were analyzed by gas chromatography, also using octan-1-ol as internal standard. The product yields were based on the amount of PhIO added to the reactions. The molar ratio 1:10 catalyst/oxidant was estimated based on molecular mass of MP including the insoluble solids catalysts. Control experiments were also carried out in the absence of MP**x** using the methodology described above.

The insoluble solids FeP**6**, MnP**6**, and CuP**6** were recovered after the first use and washed with water, methanol, acetonitrile, and dichloromethane, dried at 55 °C for 48 h, and reused in further reactions. The resulting washing solutions of all the recovered catalysts were analyzed by UV-VIS spectroscopy, to investigate the presence of metalloporphyrin in any of the washing solutions of these solid catalysts.

Characterization Techniques

Electronic spectra (UV-VIS) were obtained on a Cary-Varian and Shimadzu UV-2501PC spectrophotometer, in the 350-700 nm range. Spectra of the solid samples were recorded in a 0.1 cm path length quartz cell (Hellma) in nujol mull. Transmission Fourier Transform Infrared (FTIR) spectra were registered on an FT Mattson 7000 galaxy spectrophotometer in the 400-4000 cm^{-1} range, using KBr pellets. KBr was ground with a small amount of the solid to be analyzed, and the spectra were collected with a resolution of 4 cm^{-1} and accumulation of 64 scans. ^{1}H and ^{19}F NMR spectra were recorded on a Bruker Avance 300 spectrometer at 300.13 and 282.38 MHz, respectively. Deuterated methanol, acetone, and chloroform were used as solvents; TMS (δ 0 ppm*)* was the internal standard. The chemical shifts are reported in ppm (δ),

and the coupling constants (*J*) are given in Hz. Mass spectra were acquired on a 4800 Proteomics Analyzer mass spectrometer (MALDI TOF/TOF), and HRMS were recorded on VG AutoSpec Q and M mass spectrometers. Electron paramagnetic resonance (EPR) measurements of the powder materials were accomplished on an EPR BRUKER EMX microX spectrometer (frequency X, band 9.5 GHz), at room temperature and 77 K (using liquid N_2), using perpendicular microwave polarization X-band. Analyses at 77 K parallel microwave polarization X-band EPR experiments were conducted on a Bruker Elexsys E500 spectrometer equipped with a Bruker ER4116DM dual mode resonator. Products from the catalytic oxidation reactions were quantified using a gas chromatograph Agilent 6850 (FID detector) equipped with a DB-WAX capillary column (J&W Scientific). Quantitative analysis was accomplished by the internal standard method.

3. Results and discussion

*3.1. Synthesis of porphyrin derivatives P**2**-P**6** from the reaction of P**1** with 4-mercaptobenzoic acid*

The synthesis of the free-base porphyrins P**2**-P**6** (Figure 1) relied on the well-established reactivity of the *p*-fluorine atoms in the presence of nucleophiles [48,49]. Sulfur-containing derivatives like thiols constitute excellent nucleophiles for this type of functionalization. Indeed, the first synthesis reported in the 1990s involved the reaction between the zinc(II) complex of [H_2(TPFPP)] with butane-1-thiol, to give the corresponding tetra-substituted metalloporphyrin in 85% yield [28,51].

Here, it was reacted porphyrin P**1** with 4-mercaptobenzoic acid (MERC) previously treated with pyridine in DMF, at room temperature. The yields of mono-

(P**2**), di- (P**3** and P**4**), tri- (P**5**), and tetra- (P**6**) substituted porphyrins (Figure 1) depended on the reaction time and on the amount of 4-mercaptobenzoic acid.

After 1 h of reaction, a MERC/P**1** molar ratio of 4:1 preferentially afforded the mono-substituted porphyrin P**2** (34% yield), along with porphyrins P**3** and P**4** in yields ranging from 15 to 25% and unreacted porphyrin P**1** (20%). Under the same conditions but using a reaction time of 3 h, it was possible to isolate all the porphyrins as a complex mixture of P**2**, P**3**, P**4**, P**5**, and P**6** in 19%, 17%, 12%, 37%, and 3% yield, respectively. It was successfully optimized the formation of the tetra-substituted porphyrin P**6** to 96% yield by performing the reaction in the presence of large excess of 4-mercaptobenzoic acid (0.7 mmol) relative to the amount of porphyrin P**1** (0.1 mmol), using 4.0 mL of pyridine and extending the reaction time to 48 h.

After purification by preparative TLC, all the new compounds was characterized by UV–VIS and FTIR spectroscopies, ^{1}H and ^{19}F NMR, and high-resolution mass spectrometry (HRMS, FAB^{+}) (see experimental part and Supporting information-Figures S1- S12). As expected, the less polar fraction (higher R_f) corresponded to the mono-substituted derivative P**2**, which bore a single MERC group. The two fractions that came just behind and had very close R_f referred to the di-substituted derivatives P**3** and P**4**, followed by the tri-substituted P**5**, and finally by the most polar fraction, the tetra-substituted P**6**. The attribution of **P3** (trans) and **P4** (cis) was made in accordance with the expected polarity [34].

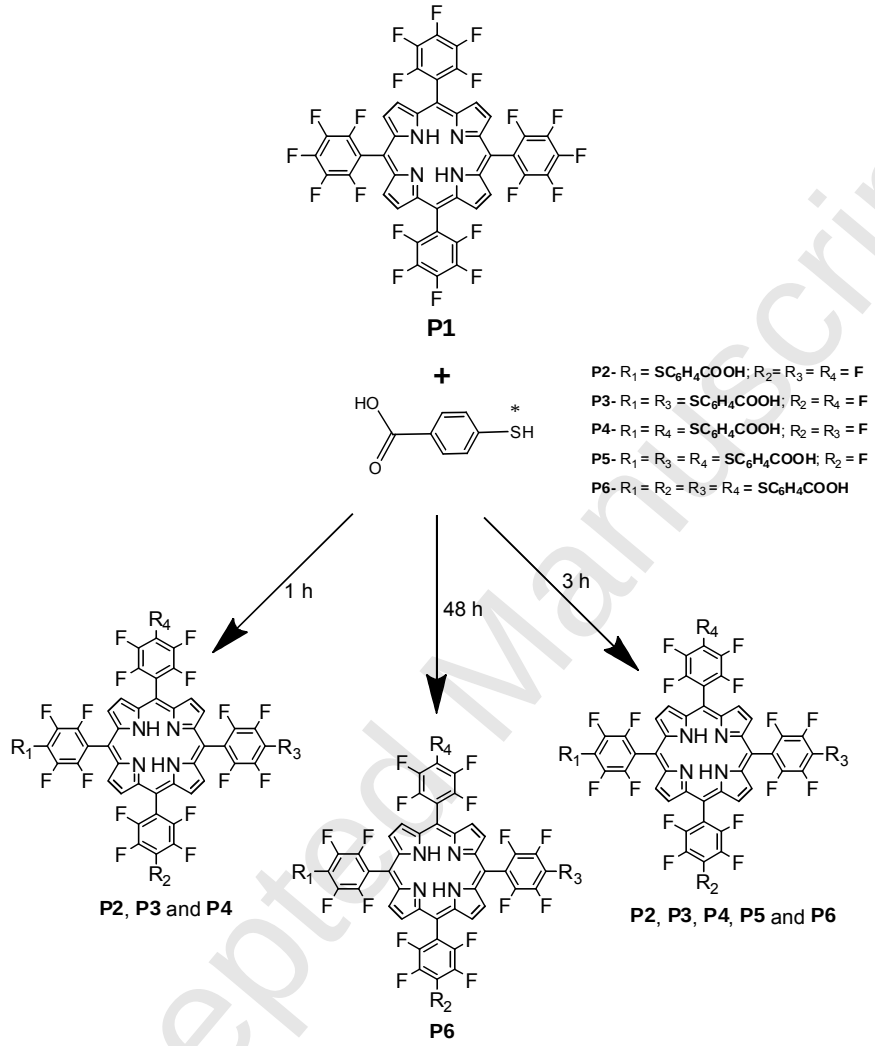

Figure 1. Schematic representation of the reactions between porphyrin P**1** and 4-mercaptobenzoic acid (MERC), to obtain the derivatives P**2** - P**6**.

The ^{1}H NMR spectra of the new porphyrins showed the appearance of two characteristic signals in the aromatic region: in the region of δ 7.65-7.68 ppm shaped doublet (J = 8.4 Hz, 2H) and one doublet in the region of δ 8.05 to 8.08 ppm (J = 8.4

Hz, 2H), corresponding to resonance of protons S-R and R-CH=CH-CO_2H, respectively. This is a direct evidence of MERC presence in the derived products.

The new porphyrins P**2**-P**6** exhibited the typical FTIR bands of free-base porphyrins, in addition to the bands characteristic of MERC binding to porphyrin P**1** at 3438 cm^{-1} (OH stretching) and at 1694 and 1486 cm^{-1} (C=O stretching) (Supporting information-Figure S11).

The UV–VIS spectra of porphyrins P**2**-P**6** presented slightly broader bands as compared with the bands observed for porphyrin P**1**, attributed to the presence of the new substituents (Supporting information-Figure S12). The highly successful "four-orbital" model explains the origin and the number of bands observed in the spectra of the free-base porphyrins [52]: changes in the porphyrin ring can affect the UV–VIS absorption spectrum, so the broadened Soret band of the new compounds (P**2**-P**6**) may stem from greater interaction of the substituted phenyl groups with the porphyrin ring and/or from some intermolecular aggregation.

*3.2. Preparation of manganese, iron, and copper porphyrins (MP**x**)*

To obtain the Fe(III) and Mn(III) complexes of porphyrins P**2** and P**6** and the Cu(II) complex of P**6** for further use in the catalytic studies, we treated the free bases with the appropriate iron(II), manganese(II), or copper(II) salts under conventional conditions. As expected, the free-base porphyrin P**2** afforded the corresponding complexes FeP**2** and MnP**2** (Figure 2), which were soluble in most organic solvents

(FeP**2** ($C_{51}H_{13}F_{19}FeN_4O_2S$): UV–VIS ($CH_3OH$) λ_{max}, nm: 412, 506 and 584; MALDI (TOF/TOF) (*m/z*):1161.9 $[M+H]^+$ and HRMS (FAB^+) (*m/z*): 1161.9800

corresponding to the calculated formula $C_{51}H_{13}F_{19}FeN_4O_2S$. MnP**2** ($C_{51}H_{13}F_{19}MnN_4O_2S$): UV–VIS ($CH_3OH$) λ_{max}, nm: 460 and 556; ESI-MS m/z: calcd for $C_{51}H_{13}F_{19}MnN_4O_2S$ (M-2H): 1158.99; found: 1158.99 - Supporting information - Figures S13, S14 and S15). The displacement of Soret band and the reduction of number of Q-bands resulted from alteration in the microsymmetry of the porphyrin macrocycle from D_{4h} to D_{2h}, a consequence of the presence of the Fe(III) or Mn(III) ion in the porphyrin core. This symmetry chance can be explained by the orbitals analysis as described by Goutermann [52].

A different situation emerged in the case of porphyrin P**6**. For the three metal ions used in this work, metal insertion into porphyrin P**6** culminated in precipitation of the resulting metalloporphyrin at the end of the reaction, which constituted an unexpected outcome indeed, metalloporphyrins do not generally precipitate in the solvent where the free-base is soluble [47]. However, the solids originating from metal insertion into porphyrin P**6** (FeP**6**, MnP**6**, and CuP**6**) exhibited a different solubility pattern from that of free-base P**6**: they were all only slightly soluble in solvents where the free-base P**6** was very soluble (e.g., DMF, THF, and acetone) as well as in other tested solvents ($CHCl_3$, CH_2Cl_2, CH_3OH, toluene, ethanol, acetonitrile, and H_2O). Compared with P**6** and MP**2**, the low solubility of MP**6** suggested formation of a structured solid as in the case of solids known as metal organic frameworks (MOFs) [53].

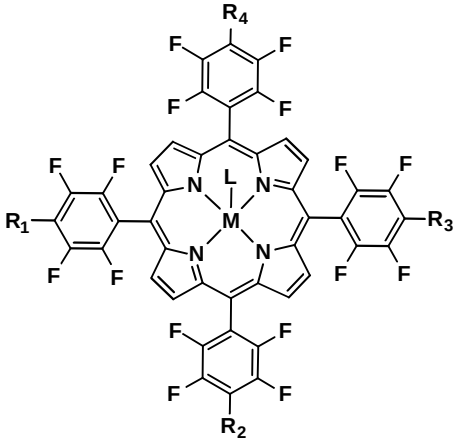

FeP1 - $R_1 = R_2 = R_3 = R_4 =$ **F**; M = Fe^{3+}
MnP1- $R_1 = R_2 = R_3 = R_4 =$ **F**; M = Mn^{3+}
CuP1- $R_1 = R_2 = R_3 = R_4 =$ **F**; M = Cu^{2+}
FeP2 - $R_1 =$ **SC_6H_4COOH**; $R_2 = R_3 = R_4 =$ **F**; M = Fe^{3+}
FeP6 - $R_1 = R_2 = R_3 = R_4 =$ **SC_6H_4COOH**; M = Fe^{3+}
MnP2 - $R_1 =$ **SC_6H_4COOH**; $R_2 = R_3 = R_4 =$ **F**; M = Mn^{3+}
MnP6 - $R_1 = R_2 = R_3 = R_4 =$ **SC_6H_4COOH**; M = Mn^{3+}
CuP6 - $R_1 = R_2 = R_3 = R_4 =$ **SC_6H_4COOH**; M = Cu^{2+}

Figure 2. Schematic representation of iron(III), manganese(III), and copper(II) porphyrins, where L represents the counter-ion (chloride or acetate) for FeP and MnP, respectively. For simplification purposes the counter-ion was omitted on the name of all compounds used in this work.

MOFs are solids that originate from binding between organic or inorganic molecules and metal clusters, which results in a robust and often nanoporous bi- or tridimensional supramolecular structure [12,54]. Supramolecular systems based on porphyrins can display various kinds of interactions: a ligand group can interconnect the macrocycles (van der Waals interactions), or one donor atom present in the metalloporphyrin can bind to the metal center of another metalloporphyrin [12].

The assumption that a structured solid arose during metal insertion into porphyrin P**6** relied on the fact that the porphyrin structure contained carboxylic acid groups. Suslick et al. [55] reported that porphyrins displaying peripheral carboxylic groups favor the formation structured solid via coordination of the carboxyl groups with the metal ions, to give rise to bi-and tridimensional structures of the solid. In a

similar way, porphyrins containing terephthalic acid as substituents in the porphyrin ring tended to form structured solid [56].

UV–VIS, FTIR, and EPR spectroscopies as well as mass spectra (Figures S14, S15, S16 and S17-Supporting information) helped to characterize the prepared metalloporphyrins. Compared with data obtained for the free-base porphyrins, the UV–VIS spectra of the metalloporphyrins confirmed insertion of the three different metal ions into porphyrin P**6** (Supporting information-Figures S12 and S13). Figure 3 depicts the UV–VIS spectra of solid MP**6** and includes the spectrum of porphyrin P**6** for comparison (in Nujol mull). The spectrum of free-base P**6** (Figure 3a) displayed Soret band in the region of 400 nm as well as the typical Q bands in the visible region, as expected for this free-base porphyrin [31]. The insoluble MP**6** presented a reduced number of bands in the visible region (from three to one, as expected), in addition to the typical Soret band of each complex. For FeP**6** and CuP**6**, the Soret band did not shift significantly. As expected, Mn(III) ion insertion into the free-base porphyrin elicited a large bathochromic shift of the Soret band [52,57,58]. In other words, the UV–VIS spectra of the solids MP**6** presented the typical bands of metalloporphyrins, attesting that the insoluble solids (FeP**6**, MnP**6**, and CuP**6**) really referred to metallated P**6**. The synthesized MP**6** probably consisted of structured solids containing metalloporphyrins as building blocks. However, despite the evidence obtained from the UV–VIS spectra and the solubility behavior, it is difficult to safely infer any structural or chemical information about the solids obtained from metal insertion into porphyrin P**6**.

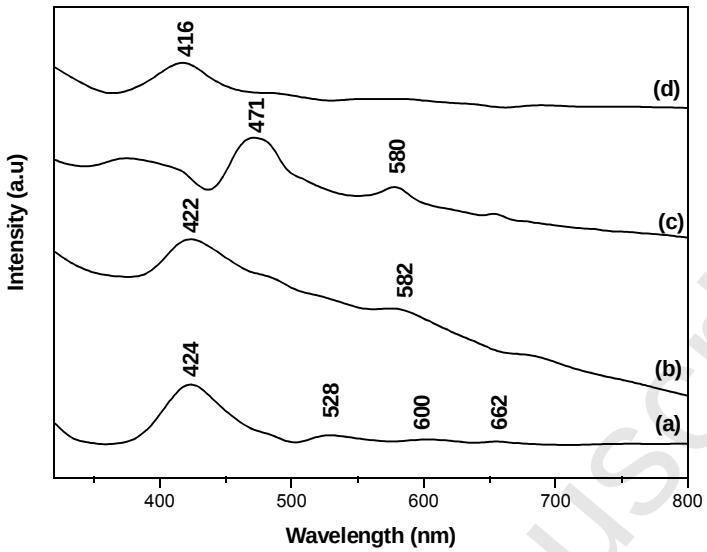

Figure 3. UV–VIS spectra of the solid samples dispersed in Nujol mull: (a) Free-base porphyrin P**6**, (b) FeP**6**, (c) MnP**6**, and (d) CuP**6**.

The EPR spectra showed that the iron porphyrins (FeP**2** and FeP**6**, Figure 4) displayed signals characteristic of high-spin Fe(III), S = 5/2, in the region of axial symmetry $g_{//}$ = 6.0, as well as a signal with low intensity in the region of g = 4.3, typical of rhombic symmetry [59-61].

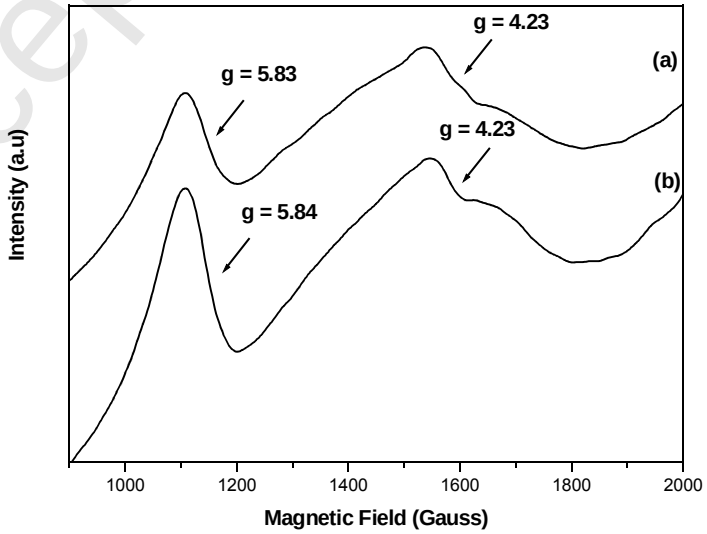

Figure 4. EPR spectra in solid sample at room temperature: (a) FeP**2** and (b) FeP**6**.

The perpendicular microwave polarization X-band EPR analysis of the MnP**2** compound was EPR silent (Figure not shown) but the solid MnP**6** revealed a broad isotropic signal in the region of g = 2.0, which can correspond to the presence of Mn(II) species. In this case, the Mn(II) ion, a system with five electrons in an environment of D_{4h} symmetry, is expected to exist. This system is paramagnetic and EPR active [62] (Supporting information- Figure S17).

Considering that the metal in MnP**2** (Soret band at 460 nm) and MnP**6** must be Mn(III), as inferred from the UV–VIS spectrum (Figure 3c), these metalloporphyrin should not have presented any EPR signals; that is, it should be EPR silent on perpendicular microwave polarization X-band EPR [63]. This absence of signal was observed for the MnP**2** EPR analysis but nevertheless, as described in the previous paragraph, an EPR signal emerged at g = 2.0 (Figure S17) for the solid MnP**6**, which could refer to the existence of Mn(II) ions that probably acted as coordinative ions for the peripheral acid groups present in the ring of porphyrin P**6**. This coordination should generate and stabilize the structured solid MnP**6** [12].

To confirm the presence of Mn(III) in MnP**2** and MnP**6** by EPR, it was used the non-conventional polarization of the microwave field, parallel to the external magnetic field. This technique shows signals corresponding to forbidden transitions; i. e., transitions with $|\Delta m_S| > 1$ [63,64]. The Zero Field interaction (ZF) present in the Mn(III) (S = 2) magnetic system causes the spin-related energy level to split into three levels. These levels correspond to the effective spin angular momenta of S = 2, S = 1, and S = 0, separated by -6D, 3D, and 6D related to the energy barycenter, respectively, for

positive values of the Zero Field Splitting parameter, *D*, which is a measure of the intensity of the ZF interaction.

Application of the parallel microwave polarization technique to MnP**2** and the solid MnP**6** evidenced the transition m_S = -2 → m_S = +2 in the lowest-energy spin level, *S* = 2. The transition corresponded to $|\Delta m_S|$ = 4 and occurred around g ~ 8.9 (750 G), as expected (Figure 5).

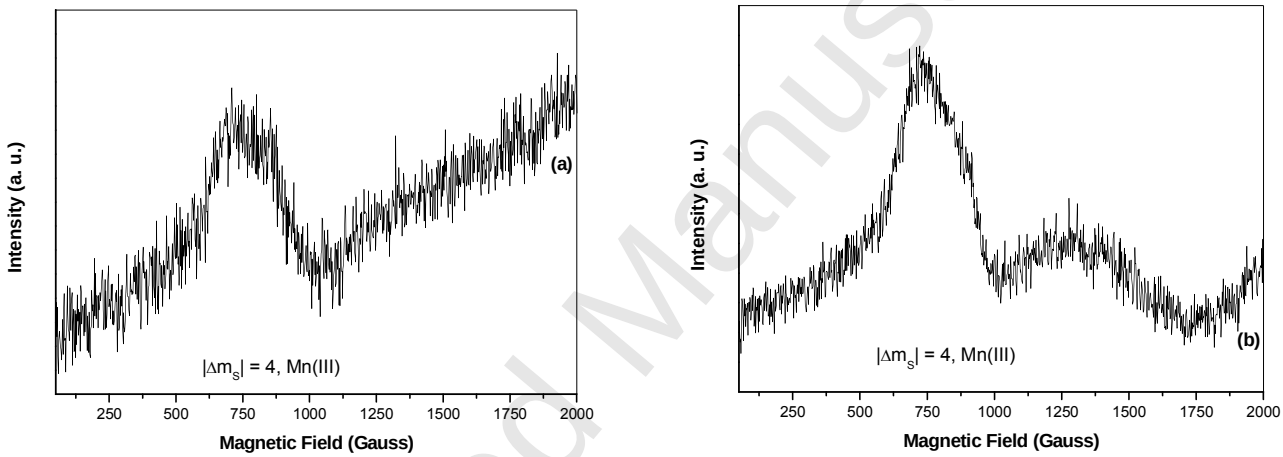

Figure 5. EPR spectra in the polarization parallel to the magnetization axis of the solid MnP samples at 77 K: (a) MnP**2** and (b) MnP**6**.

Both MnP**2** and MnP**6** exhibited a signal at g ≃ 8.9, ascribed to a transition with $|\Delta m_S|$ = 4, related to the presence of Mn(III) species (Figure 5). This suggested that both complexes contained Mn(III), which probably inserted in the inner core of porphyrins P**2** and P**6**. The presence of this signal and also the intense signal

associated with Mn(II) present in the perpendicular spectrum of solid MnP**6** (Figure S17) suggested that the Mn(II) ion might play a structuring function in the metalloporphyrin Mn(III)P**6**, to give structured solid MnP**6**, which is responsible by the high insolubility of this solid in comparison to MnP**2**.

The Cu^{2+} ion presents a d^9 electronic configuration with one unpaired electron. This makes the EPR technique a valuable tool to investigate copper complexes [65]. The EPR spectrum of Cu(II) provides valuable information regarding the oxidation state, binder type, and symmetry of copper compounds. Cu(II) is an S=1/2 system, but ^{63}Cu and ^{65}Cu nuclei have a nuclear spin of I=3/2, which gives rise to the hyperfine splitting between the unpaired electron and the nucleus itself. Thus, the EPR spectrum of a Cu(II) complex consists of four lines with large g in the region of 2.0 [65,66]. The EPR spectrum of solid CuP**6** (Figure 6a) presented the characteristic anisotropic signal for Cu(II), S = 3/2, in axial symmetry in the region around g = 2.0.

To investigate the solubilization behavior of the insoluble solid CuP**6**, we dissolved a sample of this solid in a solution of acetic acid (2 mol/L) and evaporated it to dryness, to obtain another solid, designated CuP**6**-d. The EPR spectrum of CuP**6**-d (Figure 6b) displayed the typical EPR pattern of Cu(II), accompanied by a multiple line pattern in the perpendicular region of the spectrum. The latter pattern is characteristic of super-hyperfine interaction of the copper ion unpaired electron with four magnetically equivalent ^{14}N nucleus (I=1). The appearance of these signals in the EPR spectrum of the solid CuP**6**-d suggested that the previously structured solid CuP**6** probably broke in the presence of acid. This might have occurred via a protonation process or de-coordination of metal ions, to give CuP**6** in solution as well as free copper ion and copper ion coordinated to acetate ions.

Interestingly, CuP**6**-d was very soluble in acetone, in contrast to solid CuP**6** (analyzed by EPR as illustrated in Figure 6a), which only became soluble in acetone after being solubilized in acetic acid.

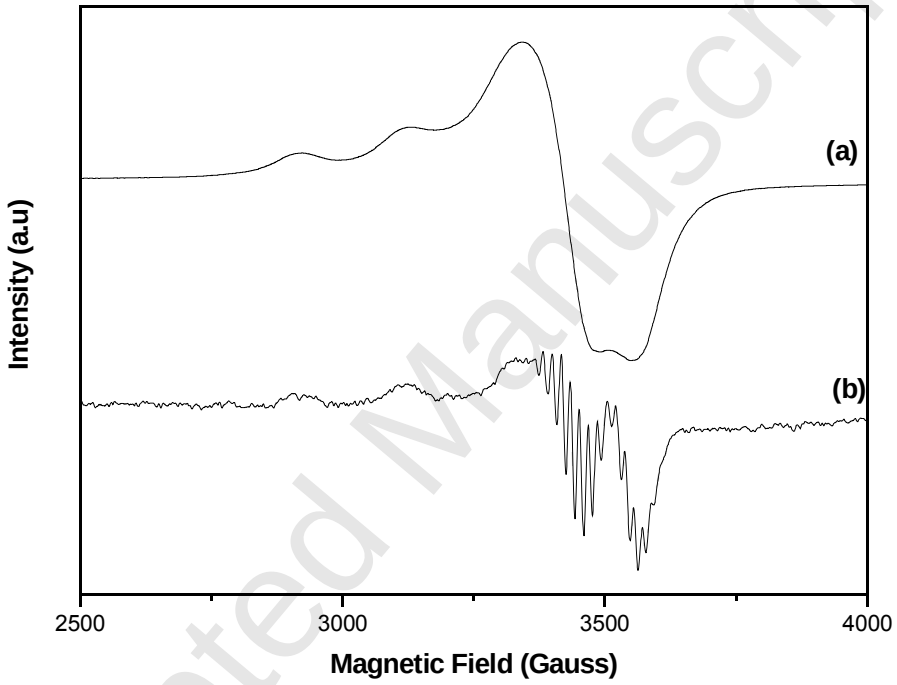

Figure 6. EPR spectra of solid samples at 77 K: (a) solid CuP**6** and (b) solid resulting from CuP**6** dissolution with acetic acid solution (2 mol/L), after evaporation of the acid solution (designated solid CuP**6**-d).

The EPR spectrum of CuP**6**-d dissolved in acetone, recorded in frozen solution (at 77 K) conditions (Figure 7a), provided better resolution of the typical Cu(II) lines of the hyperfine and super hyperfine interaction of this ion with the four nitrogen coordinative ligands of the porphyrin macrocycle. Table 1 compiles the EPR parameters obtained by simulating the experimental spectrum (Figure 7b) using the

Easyspin software package [67]. These values agreed with those obtained for metalloporphyrins with D4h symmetry (square planar) around the Cu(II) ion, as expected.

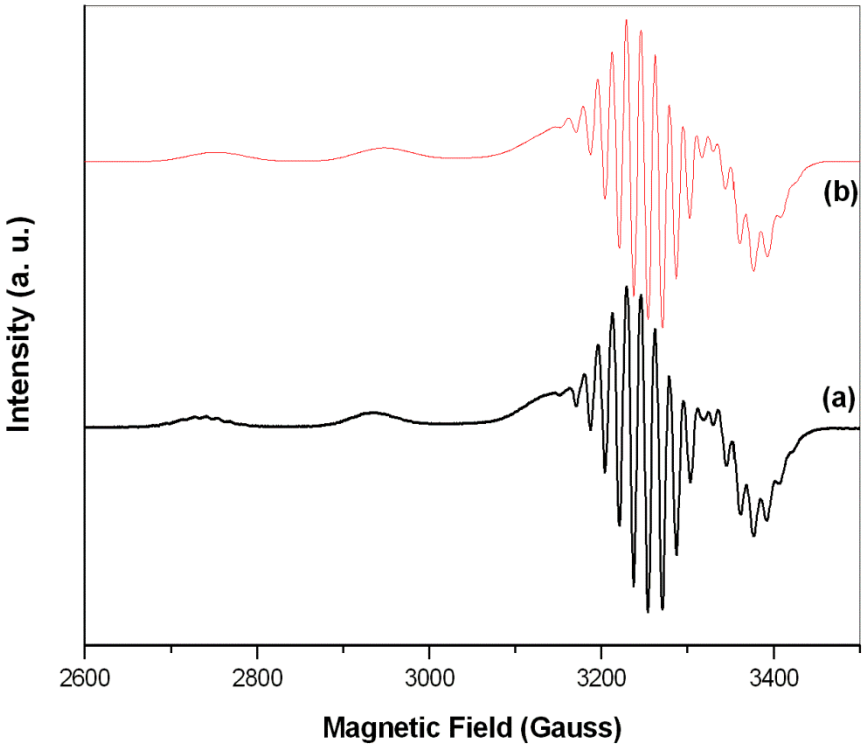

Figure 7. (a) EPR spectrum of the frozen solution (at 77 K) of the solid CuP**6**-d in acetone. (b) Simulation of the EPR spectrum.

Table 1: Spin Hamiltonian parameters for the X-band EPR spectral simulations[a] conducted for CuP6 dissolved in acetic acid solution (2 mol/L), dried, and redissolved in acetone (frozen solution EPR spectrum at 77 K) (Figure 7b).

Main direction	*g* tensor	*A* tensor [MHz]	
		$^{63, 65}$Cu	^{14}N

Perpendicular	2.05044	58.0625	45.3597
Parallel	2.20124	599.479	52.0477

[a]The EPR parameters listed in the table were obtained by simulating the experimental spectrum at 77K in acetone solution using the Easyspin pack software.

The diffractogram of the starting salt $Cu(OAc)_2$ resembled the diffraction pattern reported in the literature [68]. The PXRD pattern of CuP**6** (Figure 8b) was different from the diffraction pattern of the starting material. An intense peak arose at 2θ = 13.26°, corresponding to a distance of 6.7 Å (001). Another peak appeared at 2θ = 26.64°, relative to a short distance (around 3.35 Å) (002). Moreover, diffraction peaks emerged between 5-10º (2θ), as observed for other MOFs [69,70].

Resolvation and drying under vacuum helped to investigate the robustness of the material [69]. First, re-exposure of the CuP**6** powder to DMF induced resolvation. Then, exhaustive drying of CuP**6** under vacuum at room temperature eliminated traces of the solvent DMF. Next, analysis of the resulting solid by PXRD (Figure 8c) did not evidence any significant modifications. In fact, CuP**6** retained its crystallinity, which was consistent with the crystallinity of fresh CuP**6** and was characteristic of materials with good gas-occlusion properties [70].

Overall, the solid compounds resulting from iron, copper, and manganese insertion into porphyrin P**6** were highly insoluble. Elemental analysis of solids FeP**6**, MnP**6**, and CuP**6** were not consistent with the structure expected for molecular MP**6** complexes. The solubility of the resulting solid complexes in acidic medium suggested a break in their structure, as evidenced by detection of free tetra-substituted MP**6** in solution (structure confirmed by mass spectra (ESI-MS) as opposed to a

supramolecular structure containing MP**6** building blocks connected by metal ions coordinated to the donor atoms of the *meso*-aryl substituents (Figure S17-Supporting information). Additionally, the EPR spectrum for compound MnP**6** corroborated the presence of manganese in different oxidation state. This indicated that Mn(III) porphyrins constituted building blocks of the solid, and that Mn(II) species probably acted as construction units.

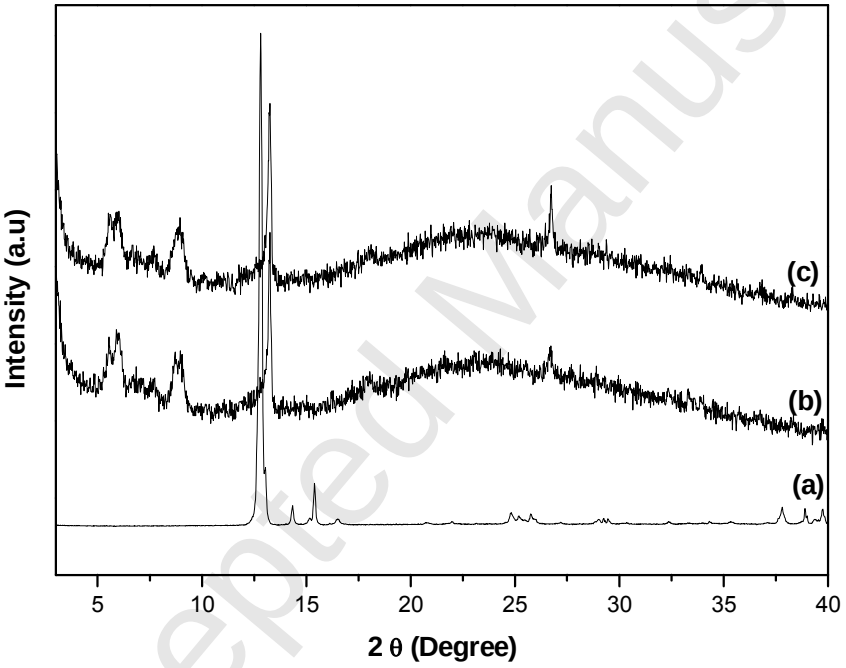

Figure 8. PXRD patterns of the solid CuP**6** indicate that crystallinity is maintained in the absence of guest molecules. (a) $Cu(AcO)_2$, (b) CuP**6**, and (c) CuP**6** after drying for 2 h and redissolution.

3.3. Catalytic oxidation reactions

The catalytic efficiency of MP**x** was evaluated under homogeneous (FeP**2** and MnP**2**) and heterogeneous (FeP**6**, MnP**6**, and CuP**6**) conditions, in the oxidation of (Z)-cyclooctene, cyclohexane, and heptane. To assess whether the presence of

MERC groups affected the well-known catalytic ability of metallocomplexes of the starting porphyrin P**1**, we also report results obtained with FeP**1**, MnP**1**, and CuP**1** [5,71-73].

To simplify the discussion and for comparison purposes, the results concerning each substrate was showed separately,. All the catalytic studies were conducted under similar reaction conditions for both the homogeneous and the heterogeneous catalytic systems.

(*Z*)-Cyclooctene

(Z)-Cyclooctene is a substrate that is easy to oxidize in reactions catalyzed by metalloporphyrins [74]. The corresponding epoxide emerges as a single product. This behavior is usually justified by the higher stability of the intermediate involved in the formation of the epoxide as compared with the intermediate leading to the eight-membered allyl radical ring [2,75,76]. The proton abstraction from the allyllic position of *cis*-cyclooctene generates a less stable radical than proton abstraction from the vinyllic position. The allylic radical acquires an unfavorable configuration due *trans* interactions that can occur between the hydrogen atoms. To maintain the unsaturation and the radical structure in the same plane, the chain of allylic radical becomes distorted and, thus, less stable.

Table 2 summarizes the catalytic results obtained in the epoxidation of (Z)-cyclooctene in the presence of MP**2** (FeP**2**, MnP**2**), MP**6** (FeP**6,** MnP**6**, and CuP**6**), and MP**1** (FeP**1,** MnP**1**, CuP**1**). This same table compiles the recycling studies carried out with the series of insoluble solids MP**6**.

The catalytic tests confirmed the expected efficiency of MP**1** [31,72,76] in the oxidation of (Z)-cyclooctene. The epoxide yields decreased in the following order: FeP**1** ~ MnP**1** > CuP**1**.

The epoxide yield obtained in the presence of FeP**2** was similar to that observed for FeP**1** (Table 2, run 4 versus run 1), which suggested that substitution of one of the electronegative *p*-fluorine atom by the bulky MERC group did not affect the stability of the porphyrin core [5] and still favored the formation of the active catalytic species [2]. The high stability of FeP**2** in solution probably stemmed from the presence of the acid group, which may have facilitated bi-molecular interactions.

Table 2: (Z)-cyclooctene oxidation by PhIO catalyzed by MPx in homogeneous[a] and heterogeneous[b] media.

Catalyst	Run	Epoxide yield (%)[c]
FeP**1**[a]	1	100
MnP**1**[a]	2	98
CuP**1**[a]	3	80
FeP**2**[a]	4	97
FeP**6**[b]	5	75
FeP**6**[b] first reuse	6	67
FeP**6**[b] second reuse	7	67
FeP**6**[b] third reuse	8	63
FeP**6**[b] fourth reuse	9	63
FeP**6**[b] fifth reuse	10	58

MnP**2**[a]	11	77
MnP**6**[b]	12	54
MnP**6**[b] first reuse	13	56
MnP**6**[b] second reuse	14	53
MnP**6**[b] third reuse	15	58
MnP**6**[b] fourth reuse	16	56
MnP**6**[b] fifth reuse	17	57
CuP**6**[b]	18	60
CuP**6**[b] first reuse	19	55
CuP**6**[b] second reuse	20	52
CuP**6**[b] third reuse	21	51
CuP**6**[b] fourth reuse	22	50
CuP**6**[b] fifth reuse	23	41
PhIO[d]	24	12

[a,b]The cyclooctene oxide yield was calculated on the basis of the amount of PhIO used in each reaction. The catalytic results represent an average of at least duplicate reactions. MP**x**/PhIO/(Z)-cyclooctene molar ratio = 1:10:1000. Reaction time: 1 h. [c]Cyclooctene oxide. [d]control reaction with no catalyst addition.

The results clearly showed the role that the metal played in the catalytic efficiency of this series of MP**x**. For the mono-substituted metalloporphyrin series, FeP**2** performed better than MnP**2** (97% versus 77 % epoxide yield, runs 4 and 12, respectively), which indicated that the iron catalytic species was more stable than the manganese one.

As for the insoluble tetra-substituted metalloporphyrin series, again the iron complex FeP**6** (75% epoxide yield, Table 2, run 5) was more efficient than the manganese complex MnP**6** (54% epoxide yield, Table 2, run 12). These results attested to the presence of Fe(III) and Mn(III) in the porphyrinic core of the solids FeP**6** and MnP**6**. The copper complex CuP**6** was also catalytically efficient (60% epoxide yield, Table 2, run 10).

In general, Mn(III)Ps bearing electron-withdrawing and electron-donating substituents are more efficient than the parent Fe(III)Ps. Nakagaki et al. attributed this fact to less effective overlap of the filled iron orbitals with the empty porphyrin orbitals as compared with the overlap involving manganese and the porphyrin orbitals [75,77]. However, Assis et al. [78] observed that FeP**1** was more efficient than the corresponding MnP and attributed this fact to the presence of Mn(II) in the catalyst. Indeed, the EPR characterization of the new complexes prepared here revealed the presence of Mn(II) in MnP**6**. Safari and Khavasi [79] compared the catalytic activity of some MnPs and FePs in two different solvents using H_2O_2, *m*-CPBA, and *tert*-butylhydroperoxide as oxidants; these authors showed that FePs displayed higher catalytic activity than MnPs at low catalyst concentration. However, in the presence of larger amounts of MnP, the product yields were similar to those obtained with the parent FeP.

The better cyclooctene oxide yields obtained in the presence of the mono-substituted complexes (FeP**2** and MnP**2**) as compared with the yields achieved in the presence of tetra-substituted (FeP**6** and MnP**6**) metalloporphyrins under the same reaction conditions were probably associated with the insolubility of MP**6** in the reaction medium. This fact may have made the access of the reagents to the metal

center of the structured solid more difficult. However, the reduced efficiency of MP**6** was largely compensated by the results from the recycling experiments conducted with the tetra-substituted series (Table 2, runs 6-10 for FeP**6**, 14-17 for MnP**6**, and 19-23 for CuP**6**). The solids MP**6** were insoluble in the reaction medium; UV–VIS monitoring of the reaction did not identify any traces of MP**6** in the reaction solvent or the washing solutions resulting from the filtration of the catalyst. This fact allowed us to conclude that MP**6** did not dissolve in the reaction medium after the first use or during the washing process, so it really constituted a heterogeneous catalyst.

After recovery and re-use of the solid catalysts MP**6**, the epoxide yield decreased only slightly. Therefore, it was possible to efficiently recycle this series of catalysts. Only after the fifth reuse did the solid CuP**6** present slightly diminished activity. This was probably associated with possible coordination of the reaction product to the metal center, or to rearrangement of the structure, which hindered access of the reactants to the catalytic site or partially inactivated the catalyst. Nonetheless, the catalytic activity of CuP**6** remained virtually the same for at least four runs (Table 2).

Cyclohexane

Compared with cyclic alkenes, cyclohexane is a less reactive substrate. Its catalytic oxidation in the presence of metalloporphyrins affords cyclohexanol and cyclohexanone as the major products; alcohol is usually the preferential product [76,80,81]. Figure 9 summarizes the results obtained in the oxidation of cyclohexane in the presence of the different catalysts synthesized in this work. The data obtained in the cases of FeP**1**, MnP**1**, and CuP**1** revealed the high selectivity of these catalysts for

the alcohol, as reported in the literature. The metal type strongly influenced the oxidation results. Indeed, the reaction catalyzed by CuP**1** furnished lower alcohol yield as compared with the reactions catalyzed by FeP**1** and MnP**1** [5,15,72,76,82-86].

Tetra-substitution of the *p*-fluorine atoms improved the efficiency of MnP**6** as compared with MnP**1** and MnP**2**-MnP**6** afforded the alcohol with higher selectivity (60%) as compared with MnP**1** (43%) and MnP**2** (34%). However, in the iron and copper series, this improvement was not evident.

Nappa [87] has shown that subtle alterations in the catalyst structure markedly change selectivity. The binding between the metal and the oxidant is a key factor underlying the formation of the active catalytic species [79]; hence, the metal can modulate the catalytic activity associated with the structure of the macrocycle. Concerning the oxidation of more inert substrates such as cyclohexane, Assis et al. [78] have described that the use of a co-catalyst enhances the catalytic activity of MnPs in solution; the alcohol yield is 60%. On the other hand, the presence of a co-catalyst drastically reduces the alcohol yield in the case of FeP**1**, from 90 to 65%. In FePs, the Fe(III) ion tends to form hexacoordinated complexes; i.e., imidazole coordinates to the two axial positions in FeP, making the formation of the active catalytic species more difficult [78].

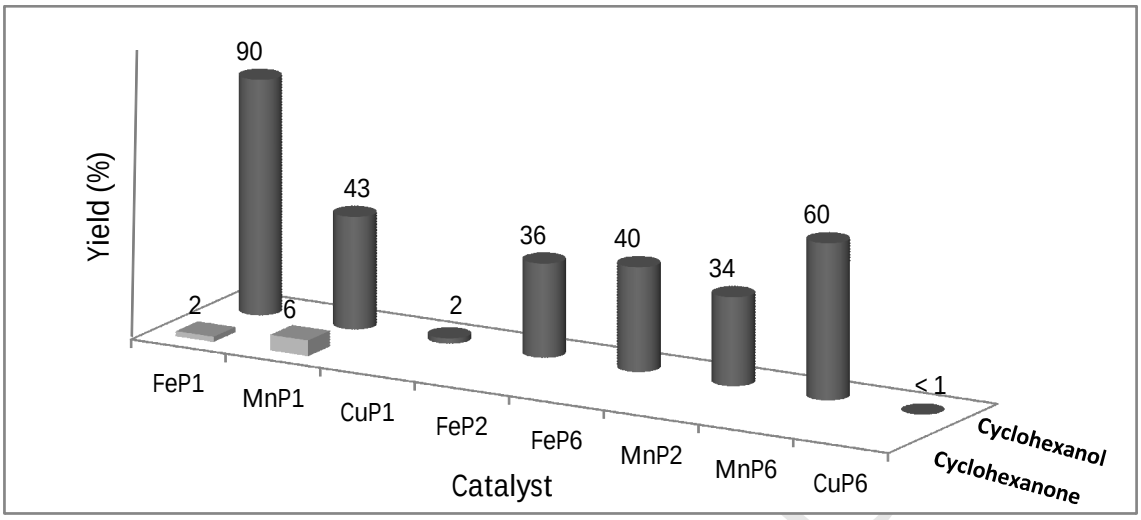

Figure 9. Cyclohexane oxidation by PhIO catalyzed by MPx in homogeneous and heterogeneous media.

Under heterogeneous conditions, the rise in product yields in the presence of a co-catalyst is not significant [78]. This probably accounted for the better performance of solid MnP**6** as compared with MnP**2** and MnP**1** in solution and in the absence of a co-catalyst. The tetra-substituted FeP**6** (alcohol yield = 40%) also performed slightly better as compared with the mono-substituted FeP**2** (alcohol yield = 36%), although the increase in yield was less pronounced than in the case of MnP**6** and MnP**2**. The mono-substituted metalloporphyrins furnished similar results (FeP**2** and MnP**2**; alcohol yield = 36 and 34%, respectively), suggesting that the metal exerted less influence in the oxidation of a more inert substrate. The data from Figure 9 suggested that the best performance of the solid MP**6** resulted from the structure of the tetra-substituted metalloporphyrins. The possible presence of channels in the micro- or mesopores of the structured solid MP**6** may have increased exposure of cyclohexane to the active center, thereby improving the reaction rate and the product

yields [88].

The great advantage of using structured solids, such as MOFs, as catalysts [11] is the fact that the solid catalyst makes the catalytic process heterogeneous while still providing the benefits of homogeneous catalysis; in this case, each part of the solid catalyst contains the metalloporphyrin. This situation does not occur for the solids prepared by catalyst heterogenization on an inert matrix, as in the case of homogeneous metalloporphyrins immobilized onto a silica support. Additionally, as observed in the case of (Z)-cyclooctene epoxidation, it may be possible to reuse all the MP**x**.

Heptane

In recent years, researchers have developed many catalytic systems based on metalloporphyrins to oxidize linear alkanes. However, only a few systems have been catalytically efficient to generate the alcohol and ketone products as well as regioselective toward the terminal positions [89]. As catalysts for heptane oxidation in homogeneous medium, metalloporphyrins preferentially produce 2-heptanol and 3-heptanol [13,90], a result of both statistical (alcohol at positions 2 and 3) and energy (alcohol at positions 1 and 4) factors [90]. Regioselectivity follows the order 3-ol ~2-ol> 4-ol >> 1-ol. Product distribution is based on the positions and number of carbon atoms in the chain.

Figure 10 illustrates the results obtained in the oxidation of heptane in homogeneous (FeP**1**, FeP**2**, MnP**1**, and MnP**2**) and heterogeneous conditions (FeP**6**, MnP**6** and CuP**6**). In all the cases, selectivity was higher for the alcohol, as observed for cyclohexane oxidation.

As in the case of cyclohexane oxidation, MP**1** afforded good yields. Although FeP**1** furnished slightly lower yields than MnP**1**, it was more selective for alcohol. As for MP**2**, they provided even higher yields than MP**1** (Figure 10).

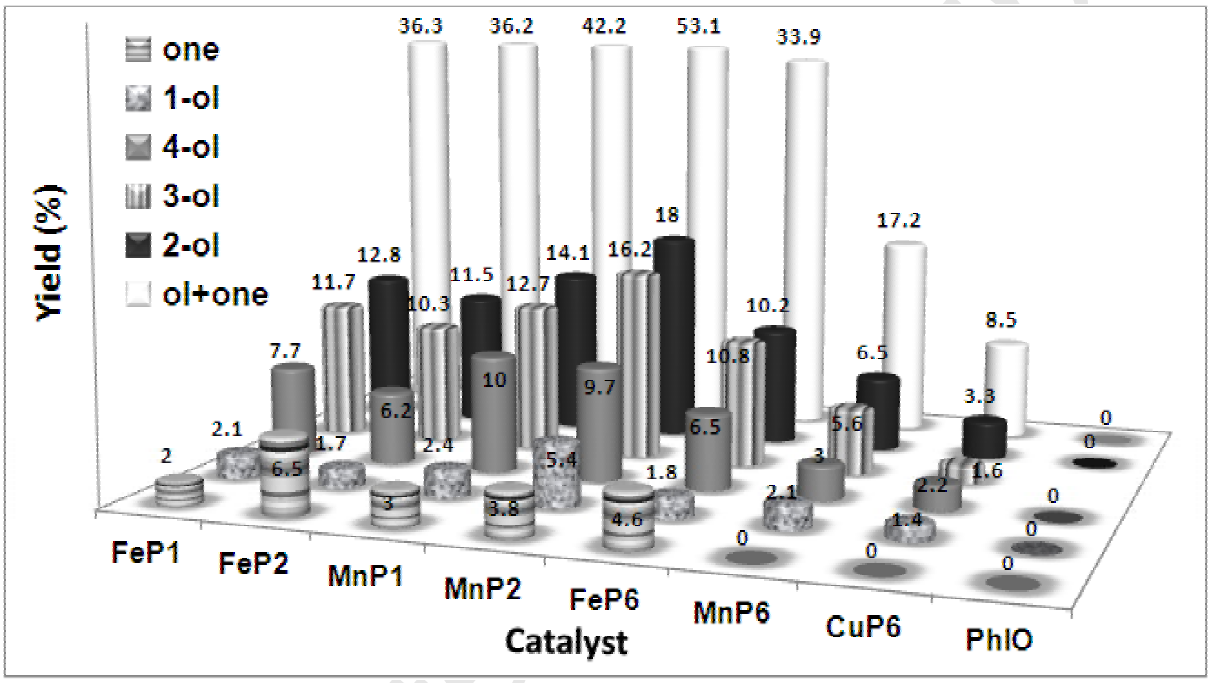

Figure 10. Results obtained in the oxidation of heptane by PhIO catalyzed by MP**x** in homogeneous and heterogeneous catalysis after 1 h of reaction. Products: one = 2-heptanone + 3-heptanone; 1-ol = 1-heptanol; 2-ol = 2-heptanol; 3-ol = 3-heptanol, and 4-ol = 4-heptanol.

The alcohol yields presented in Figure 10 were statistical for all the catalysts, with the preferential formation of 2-ol and 3-ol, followed by 4-ol >> 1-ol. The oxidation at positions 2, 3, and 4 was equivalent from the viewpoint of catalytic species formation. However, there were two positions 2 and 3 against only one position 4, so formation of products at positions 2 and 3 was statistically more favorable [90,91]. In

this sense, the 2- and 3-heptanol yields should be similar, and the 4-heptanol yield should be half the 2- and 3-heptanol yields. As for 1-heptanol, yields should be lower, because primary C–H bonds are less reactive.

The mono-substituted catalysts (FeP**2** and MnP**2**) gave higher yields as compared with the tetra-substituted complexes (FeP**6** and MnP**6**). In particular, MnP**2** performed very well in terms of efficiency and selectivity (49.3% alcohols and only 3.8% ketone) much better than FeP**2** and comparable in terms of selectivity to MnP**1**.

FeP**2** afforded yields of 29.7 and 6.5% for alcohol and ketone, respectively, which resembled the values achieved in the case of FeP**1**, although the relative ketone yield was higher for FeP**2** (12 %). MnP**2** gave a total yield of 53.1%; the yield of alcohol at position 1 was 5.4%. Substitution of the *p*-fluorine atoms with a bulkier group may account for this result.

As reported by Cook [89] in the case of heptane oxidation catalyzed by (5, 10, 15, 20-tetrakis(2',4',6'-triphenylphenyl)porphyrinato)manganese (III) acetate), [Mn(TTPPP)]OAc, in homogeneous medium, the introduction of bulky substituents can promote oxidation at the terminal positions. Nappa et al. [78] observed this same behavior when they used (5,10,15,20-tetrakis(2',4',6'-trimethoxyphenyl)porphyrinato)manganese(III) acetate), [Mn(TTMPP)], as catalyst. The introduction of bulky groups favors the approach of terminal carbons to the active catalytic center. However, the carbons at position 2 of hexane are more exposed, which explains the larger oxidation at this position. Comparable effects reported in literature, in both cases the more selectivity for terminal positions is improved to substitutions with rigid groups in the 2- and 6-position at all meso-aryl substituents. For the new compounds, the only observed improvement of the desired selectivity for 1-ol was observed

for MnP**2** compared to MnP**1**, the steric influence of a single substituent on the reaction center should be small.

To investigate the selectivity of catalysts MP**2** and MP**6** toward the carbon at position 2, we extended the reaction time to 24 h, which culminated in larger product yield (Figure 11). MnP**2** afforded 72.9% yield (alcohol = 68.4% and ketone = 4.5%), without statistical relation among the yields achieved for the various products: 2-ol > 3-ol > 4-ol > 1-ol. The 1-heptanol yield remained constant (Figures 10 and 11), and selectivity for 2-heptanol was 41% after 24 h of reaction catalyzed by MnP**2**.

Concerning FeP**6**, longer reaction time also culminated in better yields. In this case, statistical results emerged: 2-ol ~ 3-ol > 4-ol ~1-ol. Moreover, 1-heptanol yield (4.5 % versus 1.8%) increased, and ketone yields were low.

The good catalytic performance observed for FeP**6** resulted from the presence of structured FePs in the solid. As previously discussed in the section on cyclohexane oxidation, the existence of channels in a structured solid is plausible these channels facilitate exposure of the active center and the substrate approach to the catalyst. MnP**6** furnished lower 1-heptanol yields as compared with FeP**6**. This result could be attributed to the structure of the solid. The lower yield observed for MnP**6** suggested that access of the reactants to the active center was more difficult in this case, and that this catalyst required longer reaction time to oxidize a more inert substrate. In fact, longer reaction time boosted product yield while maintaining selectivity for the alcohols. This was an interesting result, because such longer reaction could have produced ketones via over-oxidation of the alcohol product. Nevertheless, even after 24 h, MnP**6** afforded lower substrate conversion than FeP**6** after 1 h.

CuP**6** performed reasonably during heptane oxidation. In general, CuPs are less reactive than MnPs and FePs. The latter catalysts have similar properties and can activate the oxidant, to generate the active catalytic species more easily. CuP**1** did not afford a significant yield during heptane oxidation (total yield < 1.0%). As for CuP**6**, total heptanol yield was 8.5%; no ketone emerged. Despite the low product yield, CuP**6** was 100% selective for alcohols, and it was able to oxidize the primary carbon (Figure 10).

The effect of introduce the 4-mercaptobenzoic acid moiety lead to higher 1-ol yields compared to the parent MP**1** compounds when the reaction time was of 24 hours. The increase in reaction time for FeP**1**, MnP**1** and CuP**1** has not led to better yields in the formation of any products (Figure not shown).

Finally, control reactions did not generate any detectable amount of products, so the catalytic activity observed in all the reactions was really due to MP**x**. The conversions, yields, and selectivities obtained with the modified MP**x** suggested that introduction of bulky groups into the structure of porphyrin P**1**, a traditional and efficient catalyst for oxidation reactions, especially when it contained iron and manganese, created a suitable environment for more selective reactions and favored oxidation of less reactive positions.

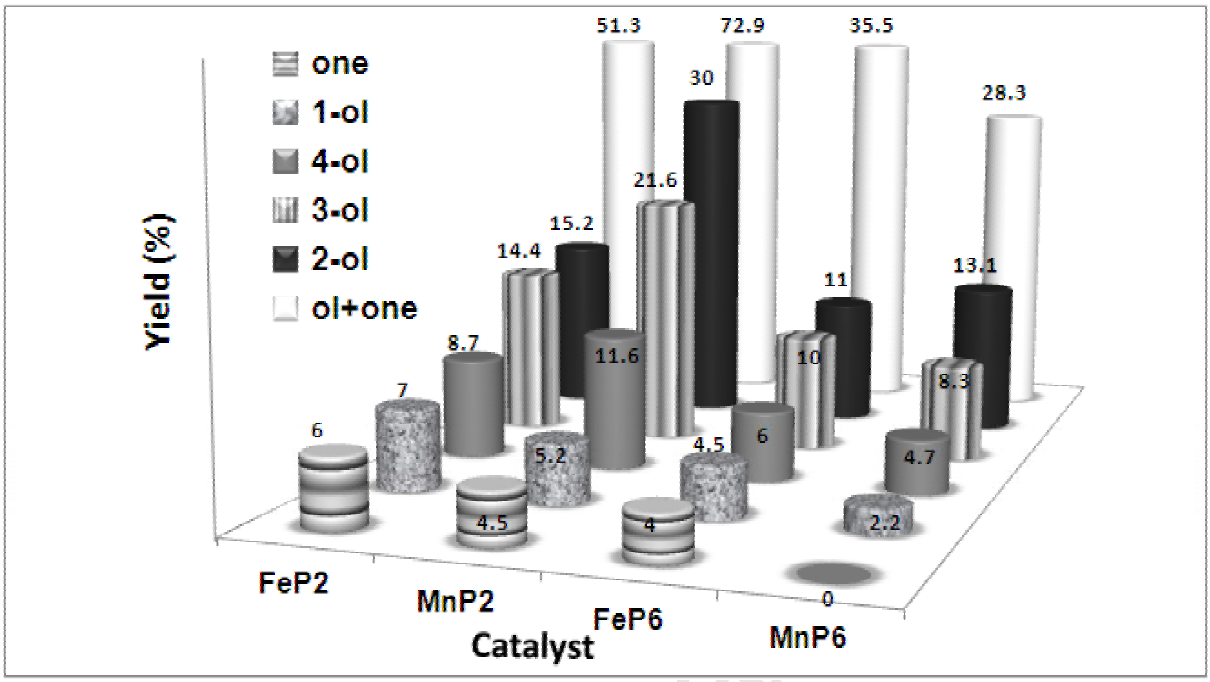

Figure 11. Results obtained in the oxidation of heptane by PhIO catalyzed by MP**x** in homogeneous and heterogeneous catalysis for 24 h. Products: one = 2-heptanone + 3-heptanone; 1-ol = 1-heptanol; 2-ol = 2-heptanol; 3-ol = 3-heptanol, and 4-ol = 4-heptanol.

The results from heptane and cyclohexane oxidation reactions catalyzed by MP**x** depended on the nature of the metal, as well as on the substituents present in the macrocycle. All the tested MP**x** were more selective for alcohols; ketone yields were low or even inexistent. Our findings are promising: insolubility of the catalysts MP**6** in the reaction medium allows for their easy recovery and reuse.

4. Conclusions

We successfully modified [H_2(TPFPP)] (P**1**) with 4-mercaptobenzoic acid, to obtain five new derivatives resulting from substitution of the *p*-fluorine atoms on the

meso-phenyl rings by reaction with the thiol group of the acid. We characterized the new compounds by UV–VIS and FTIR spectroscopies, ^{1}H and ^{19}F NMR, and HRMS. We inserted Fe(III) and Mn(III) into the mono- and tetra-substituted free-base porphyrins; we inserted copper into the tetra-substituted porphyrin. All the resulting porphyrin complexes were stable. Metalloporphyrins MP**6** were insoluble and served as catalysts in heterogeneous conditions. The new metalloporphyrins provided good to excellent yields during catalysis of (Z)-cyclooctene, cyclohexane, and heptane oxidation in homogeneous and heterogeneous media. All the metalloporphyrins were highly selective for the alcohols in cyclohexane and heptane oxidation; product profile depended on the porphyrin structure and the metal. The tetra-substituted derivatives offered the advantage of operating as heterogeneous catalysts—their reuse in (Z)-cyclooctene oxidation afforded similar results along six cycles.

Compared with MnP**1**, MnP**2** furnished higher yields in the oxidation of terminal carbons relative. FeP**6** during heterogeneous catalysis performed similarly to FeP**1** during homogeneous catalysis. However, in the former case there was an additional benefit: it was possible to recover and reuse FeP**6**.

Few literature reports have described the use of CuP as catalyst. Here, we successfully synthesized and investigated the catalytic activity of a solid based on a copper porphyrin. This solid effectively catalyzed (Z)-cyclooctene; it was also able to catalyze the oxidation of more inert substrates, albeit in modest yields.

The introduction of appropriate bulky groups into [H_2(TPFPP)] in association with the remaining electronegative atoms resulted in efficient and selective catalysts for homogeneous and heterogeneous catalysis. It was possible to modulate catalyst selectivity and efficiency by choosing the appropriate substituent and metal.

Acknowledgments

The authors are grateful to Conselho Nacional de Desenvolvimento Científico e Tecnológico (CNPq) (Project n. 471200/2012-3), Coordenação de Aperfeiçoamento de Pessoal de Nível Superior (CAPES), Fundação Araucária, Fundação da Universidade Federal do Paraná (FUNPAR), and Universidade Federal do Paraná (UFPR) for financial support. The authors also thank Fundação para Ciência e Tecnologia (FCT, Portugal), European Union, QREN, FEDER, and COMPETE for funding of the QOPNA research unit (project PEst-C/QUI/UI0062/2013; FCOMP-01-0124-FEDER-037296). The Portuguese National NMR Network also supported this work via funds from FCT. Kelly A. D. F. Castro also thanks CAPES for the PhD sandwich and CNPq for the posdoc scholarship (Proc n. 6883-10-9 and 500257/2013-2 respectively).

References

[1] A. J. Appleton, S. Evans, J. R. L. Smith, J. Chem. Soc. Perkin Trans. 2 (1995) 281-285.

[2] J. T. Groves, J. Inorg. Biochem. 100 (2006) 434-447.

[3] D. Mansuy, C. R. Chimie 10 (2007) 392-413.

[4] B. Meunier, S. P. Visser, S. Shaik, Chem. Rev. 104 (2004) 3947-3980.

[5] D. Dolphin, T. G. Traylor, L. Y. Xie, Acc. Chem. Res. 30 (1997) 251-259.

[6] J. T. Groves, T. E. Nemo, R. S. Myers, J. Am. Chem. Soc. 101 (4) (1979) 1032-1033.

[7] M. M. Q. Simões, R. De Paula, M. G. P. M. S. Neves, J. A. S. Cavaleiro, J. Porphyrins Phtalocyanines 13 (2009) 589-596.

[8] R. Paula, M. M. Q. Simões, M. G. P. M. S. Neves, J. A. S. Cavaleiro, J. Mol. Catal. A: Chem. 345 (2011) 1-11.

[9] G. F. Silva, D. C. Silva, A.S. Guimarães, E. Nascimento, J. S. Rebouças, M. P. Araujo, M. E. M. D. Carvalho, Y. M. Idemori, J. Mol. Catal. A: Chem. 266 (2007) 274-283.

[10] W. Nam, H. J. Lee, So-Young Oha, C. Kimb, H. G. Jang, J. Inorg. Biochem. 80 (2000) 219-225.

[11] K. S. Suslick, P. Bhyrappa, J. –H. Chou, M. E. Kosal, S. Nakagaki, D. M. Smithhenry, S. R. Wilson, Acc. Chem. 38 (2006) 283-291.

[12] S. Nakagaki, G. K. B. Ferreira, G. M. Ucoski, K. A. D. F. Castro, Molecules 18 (2013) 7279-7308.

[13] G. K. B. Ferreira, K. A. D. F. Castro, G. S. Machado, R. R. Ribeiro, K. J. Ciuffi, G. P. Ricci, J. A. Marques, S. Nakagaki, J. Mol. Catal. A: Chem. 378 (2013) 263-272.

[14] P. Battioni, E. Cardin, M. Louloudi, B. Schollhorn, G. A. Spyroulias, D. Mansuy, T. G. Traylor, Chem. Commun. (1996) 2037-2038.

[15] G. R. Friedermann, M. Halma, K. A. D. F. Castro, F. L. Benedito, F. G. Doro, S. M. Drechsel, A. S. Mangrich, M. D. Assis, S. Nakagaki, Appl. Catal. A: Gen. 308 (2006) 172-181.

[16] C. M. B. Neves, M. M. Q. Simões, I. C. M. S. Santos, F. M. J. Domingues, M. G. P. M. S. Neves, F. A. A. Paz, A. M. S. Silva, J. A. S. Cavaleiro, Tetrahedron Letters 52 (2011) 2898-2902.

[17] R. Ricoux, Q. Raffy, J. P. Mahy, C. R. Chimie 10 (2007) 684-702.

[18] T. L. Poulos, Biochem. Biophys. Res. 338 (2005) 337-345.

[19] J. R. Lindsay Smith, Y. Iamamoto, F. S. Vinhado, J. Mol. Catal. A: Chem. 252 (2006) 23-30.

[20] N. A. Stephenson, A. T. Bell, J. Am. Chem. Soc. 127 (2005) 8635-8643.

[21] E. H. Schaab, A. E. M. Crotti, Y. Iamamoto, M. J. Kato, L. V. C. Lotufo, N. P. Lopes, Biol. Pharm. Bull. 33 (2010) 912-916.

[22] J. T. Groves, T. E. Nemo, J. Am. Chem. Soc. 105 (1983) 6243-6248.

[23] R. J. Abraham, I. Marsden, Tetrahedron 48 (1992) 7489-7504.

[24] H. Lu, P. Zhang, Chem. Soc. Rev. 40 (2011) 1899-1909.

[25] N. A. Stephenson, A. T. Bell, J. Am. Chem. Soc. 127 (2005) 8635-8643.

[26] M. Costas, K. Chen, L. Que Jr, Coord. Chem. Rev. 200-202 (2000) 517-544.

[27] M. Linhares, S. L. H. Rebelo, M. M. Q. Simões, A. M. S. Silva, M. G. P. M. S. Neves, J. A. S. Cavaleiro, Appl. Catal. A: General 470 (2014) 427-433.

[28] S. L. H. Rebelo, M. Linhares, M. M. Q. Simões, A. M. Silva, M. G. P. M. S. Neves, J. A. S. Cavaleiro, C. Freire, J. Catal. 315 (2014) 33-40.

[29] S. M. G. Pires, M. M. Q. Simões, I. C. M. S. Santos, S. L. H. Rebelo, M. M. Pereira, M. G. P. M. S. Neves, J. A. S. Cavaleiro, Appl. Catal. A: General 439-440 (2012) 51-56.

[30] D. Mansuy, Pure Appl. Chem. 62 (1990) 741-766.

[31] P. Battioni, O. Brigaud O, H. Desvaux, D. Mansuy, T. G. Traylor, Tetrahedron Lett. 32 (1991) 2893-2896.

[32] L. B. Bolzon, H. R. Airoldi, F. B. Zanardi, J. G. Granado, Y. Iamamoto, Microporous Mesoporous Mat. 168 (2013) 37-45.

[33] K. J. Ciuffi, H. C. Sacco, J. C. Biazzotto, E. A. Vidoto, O. R. Nascimento, C. A. P. Leite, O. A. Serra, Y. Iamamoto, J. Non-Cryst. Sol. 273 (2000) 100-108.

[34] K. A. D. F. Castro, M. M. Q. Simões, M. G. P. M. S. Neves, F. Wypych, J. A. S. Cavaleiro, S. Nakagaki, Catal. Sci. Technol. 4 (2014) 129-141.

[35] J. M. M. Rodrigues, A. S. F. Farinha, P. V. Muteto, S. M. Woranovicz-Barreira, F. A. Almeida Paz, M. G. P. M. S. Neves, J. A. S. Cavaleiro, A. C. Tomé, M. T. S. R. Gomes, J. L. Sessler, J. P. C. Tomé, Chem. Commun. 50 (2014) 1359-1361.

[36] D. C. S. Costa, M. C. Gomes, M. A. F. Faustino, M. G. P. M. S. Neves, A. Cunha, J. A. S. Cavaleiro, A. Almeida, J. P. C. Tomé, Photochem. Photobiol. Sci., 11 (2012) 1905-1913.

[37] L. M. O. Lourenço, M. G. P. M. S. Neves, J. A. S. Cavaleiro, J. P. C. Tomé, Tetrahedron 70 (2014) 2681-2698.

[38] E. Alves, M. A. F. Faustino, M. G. P. M. S. Neves, A. Cunha, J. Tomé, A. Almeida, Future Medicinal Chemistry 6 (2014) 141-164.

[39] A. Tavares, S. R. S. Dias, C. M. B. Carvalho, M. A. F. Faustino, J. P. C. Tomé, M. G. P. M. S. Neves, A. C. Tomé, J. A. S. Cavaleiro, A. Cunha, N. C. M. Gomes, E. Alves, A. Almeida, Photochem. Photobiol. Sci., 10 (2011) 1659-1669.

[40] C. M. B. Carvalho, A. T. P. C. Gomes, S. C. D. Fernandes, A. C. B. Prata, M. A. Almeida, M. A. Cunha, J. P. C. Tomé, M. A. F. Faustino, M. G. P. M. S. Neves, A. C. Tomé, J. A. S. Cavaleiro, Z. Lina, J. P. Rainhod, J. Rocha, J. Photochem. Photobiol. B: Biology 88 (2007) 112-118.

[41] J-L. Zhang, J-S. Huang, C-M. Che, Chem. Eur. J. 12 (2006) 3020-3031.

[42] R. N. Silva, A. C. Tomé, J. P. C. Tomé, M. G. P. M. S. Neves, M. A. F. Faustino, J. A. S. Cavaleiro, A. Oliveira, A. Almeida, A. Cunha Microbiology and Immunology 56 (2012) 692-699.

[43] L. Costa, M. A. F. Faustino, M. G. P. M. S. Neves, A. Cunha, A. Almeida, 4 Viruses (2012) 1034-1074.

[44] J. C. Sharefkin, H. Saltzmann, Org. Synth 43 (1963) 62-62..

[45] A. M. R. Gonsalves, J. M. T. B. Varejão, M. M. Pereira, J. Heterocycl. Chem. 28 (1991) 635-640.

[46] R. De Paula, D. Pinto, M. A. F. Faustino, M. G. P. M. S. Neves, J. A. S. Cavaleiro, J. Heterocycl. Chem. 45 (2008), 453-459.

[47] H. Kobayashi, T. Higuchi, Y. Kaizu, H. Osada, M. Aoki, Bull. Chem. Soc. Jpn. 48 (1975) 3137-3141.

[48] D. Samaroo, M. Vinodu, X. Chen, C. M. Drain, J. Comb. Chem. 9 (2007) 998-1011.

[49] J. I. T. Costa, A. C. Tomé, M. G. P. M. S. Neves, J. Cavaleiro, J. Porphyrins Phthalocyanines 15 (2011) 1116-1133.

[50] J. Králova, T. Bríza, I. Moserova, B. Dolensky, P. Vasek, P. Pouckova, Z. Kejik, R. Klaplánek, P. Martázek, M. Dvorak, V. Král, J. Med. Chem. 51 (2008) 5964-5973.

[51] S. Silva, P. M. R. Pereira, P. Silva, F. A. A. Paz, M. A. F. Faustino, J. A. S. Cavaleiro, J. Tomé, Chem. Commun. 48 (2012) 3608-3610.

[52] M. Gouterman, J. Mol. Spec. 6 (1961) 138-163.

[53] S. R. Halper, L. Do, J. R. Stork, S. M. Cohen, J. Am. Chem. 128 (2006) 15255-15268.

[54] B. J. Burnett, P. M. Barron, W. Choe, Cryst. Eng Comm. 14 (2012) 3839-3846.

[55] M. Kosal, K. S. Suslick, J. Sol. St. Chem. 152 (2000) 87-98.

[56] M. Albrecht, M. Nieger, A. Schmidt, Z Naturforschung B 67 (2012) 103-106.

[57] J. Boucher, J. Am. Chem. Soc. 92 (1970) 2725-2730.

[58] T. P. Wijesekera, D. Dolphin, Ed. R.A. Sheldon, Synthetic Aspects of Porphyrin and Metalloporphyrin Chemistry., Marcel Dekker Inc., New York, (1994), Ch. 7,193-239.

[59] R. Cammack, C. E. Cooper, "Methods in Enzimology" 227 (1993) 353-384.

[60] W. R. Hagen, Coord. Chem. Rev. 190 (1999) 209-229.

[61] M. Nakamura, Coord. Chem. Rev. 250 (2006) 2271-2294.

[62] M. T. Caudle, C. K. Mobley, L. M. Bafaro, R. Lobrutto, G. T. Yee, T. L. Groy, Inorg. Chem, 43 (2004) 506-514.

[63] K. A. Campbell, M.R. Lashley, J.K. Wyatt, M.H. Nantz, R.D. Britt. J. Am. Chem. Soc. 123 (2001) 5710-5719.

[64] M. A. Vázquez-Fernández, M.R. Bermejo, M.I. Fernández-García, G. González-Riopedre, M.J. Rodríguez-Doutón, M. Maneiro, J. Inorg. Biochem. 105 (2011) 1538-1547.

[65] Y. Nonomura, Y. Yoshitaka, N. Inoue, Inorg. Chim. Acta, 224 (1994) 181-184.

[66] J. Peisach, W. E. Blumberg, Arch. Biochem. Biophys. 165 (1974) 691-708.

[67] S. Stoll, A. Schweiger, J. Magn. Reson. 178, 2006, 42-55.

[68] J. V. Bellinia, R. Machado, M. R. Morelli, R. H. G. A. Kiminam, Mat. Res. 5 (2002) 453-457.

[69] D. W. Smithenry, S. R. Wilson, K. Suslick, Inorg. Chem. 42 (2003) 7719-7721.

[70] T. Ohmura, A. Usuki, K. Fukumori, T. Ohta, M. Ito, K. Tatsumi, Inorg. Chem. 45 (2006) 7988-7990.

[71] K. S. Suslick, Eds., K. Kadish, K. Smith, R. Guilard “The Porphyrin Handbook”, Academic Press, New York (1999) 44-131.

[72] O. J. Lima, D. P. Aguirre, D. C. Oliveira, M. A. Silva, C. Mello, C. A. P. Leite, H. C. Sacco, K. Ciuffi, J. Mater. Chem. 11 (2001) 2476-2481.

[73] D. R. Leanord, J. R. Lindsay-Smith, *J. Chem. Soc. Perkin Trans 2* (1991) 25-30.

[74] S. L. H. Rebelo, M, M. Pereira, M. M. Q. Simões, M. G. P. M. S. Neves, J. A. S. Cavaleiro, J. Catal. 234 (2005) 76-87.

[75] G. M. Ucoski, K. A. D. F. Castro, K. J. Ciuffi, G. P. Ricci, J. A. Marques, F. S. Nunes, S. Nakagaki, Appl. Catal., A 404 (2011) 404, 120-128.

[76] E.C. Zampronio, M. C. A. F. Gotardo, M. D. Assis, H. P. Oliveira, Catal. Lett. 104 (2005) 53-56.

[77] G. S. Machado, P. B. Groszewicz, K. A. D. F. Castro, F. Wypych, S. Nakagaki, J. Colloid Interface Sci. 374 (2012) 278-286.

[78] A. L. Faria, T. O. C. Mac Leod, V. P. Barros, M. Assis, J. Braz. Chem. Soc. 20 (2009) 895-906.

[79] H. R. Khavasi, N. Safari, J. Porphyrins Phthalocyanines, 2009, 15, 75-81.

[80] P. Inchley, J. R. Lindsay-Smith, R.J. Lower, New J. Chem. 13 (1989) 669-676.

[81] K. A. D. F. Castro, A. Bail, P. B. Groszewicz, G. S. Machado, W. Schreiner, F. Wypych, Appl. Catal. A: Gen. 386 (2010) 51-59.

[82] Y. Iamamoto, C. M. C. Prado, H. C. Sacco, K. J. Ciuffi, M. D. Assis, A. P. J. Maestrin, A, J. B. Melo, O. Baffa, O. R. Nascimento, J. Mol. Catal. A: Chem. 117 (1997) 259-271.

[83] Y. Iamamoto, M. D. Assis, K. .J. Ciuffi, H. C. Sacco, L. Iwamoto, A. J. B. Melo, O.R. Nascimento, C.M.C. Prado, J. Mol. Catal. A: Chem. 109 (1996) 189-200.

[84] S. Nakagaki, M. Halma, A. Bail, G. G. C. Arízaga, F. Wypych, J. Coll. Int. Sci. 281 (2) (2005) 417-423.

[85] T. G. Traylor, W. P. F. D. Bandyopadhhyay, J. Am. Chem. Soc. 111 (1989) 8009-8010.

[86] Y. Iamamoto, M. D. Assis, K. J. Ciuffi, C. M. C. Prado, B. Z. Prellwitz, M. Moraes, O. R. Nascimento, H. C. Sacco, J. Mol. Catal. A: Chem. 116 (1997) 365-374.

[87] M. J. Nappa, C.A. Tolman, Inorg. Chem. 24 (1985) 4711-4719.

[88] A. M. Shultz, O. K. Farha, J. T. Hupp, S. T. Nguyen, J. Am. Chem. Soc. 131 (2009) 4204-4205.

[89] B. R. Cook, T. S. Suslick, J. Am. Chem. Soc. 108 (1986) 7281-7286.

[90] J.M. Thomas, J.C. Hernandez-Garrido, R. Raja, R.G. Bell, Phys. Chem. Chem. Phys. 11 (2009) 2799-2825.

[91] M. A. Martinez-Lorente, P. Battioni, W. Kleemiss, J.F. Bartoli, D. Mansuy, J. Mol. Catal. A: Chem. 113 (1996) 343-353.

Graphical abstract

Synthesis of new metalloporphyrin derivatives from 5,10,15,20-tetrakis (pentafluorophenyl)porphyrin and 4-mercaptobenzoic acid for homogeneous and heterogeneous catalysis